2003 SCEC Annual Report

Project Title: Multi-Cycle Dynamics of Non-Planar Faults
Principal Investigators: David D. Oglesby and Guanshui Xu
Institution: University of California, Riverside

We have made considerable progress in our project to model the dynamics of non-planar faults over multiple earthquake cycles. In the past year, we have largely focused on the effects of multiple earthquakes on relatively simple 2D asymmetric faulting systems with an approximate method for the interseismic loading period. We use the explicit finite element method (Whirley and Engelmann, 1993; Oglesby, 1999) to model both the interseismic loading process and the rupture dynamics of these systems. While this method is well suited to modeling the short-time-scale processes of earthquake rupture and slip, its small time steps (driven by stability criteria) make it very difficult to use in modeling the long time scales (hundreds of years) in the interseismic period. Thus, as a first approximation to the loading period, we simply load the fault at a rate much beyond that of true tectonic rates. This loading method should be thought of as a means to provide realistic pre-stress fields for our sequential dynamic simulations; we are not yet modeling the actual interseismic period.

Our initial models in this project consist of long-term simulations of thust and normal faults over multiple earthquake cycles. For brevity we do not discuss these results in detail; we merely note that we find that over multiple events, a relatively stable sequence of large events separated by smaller events results. Slip in the large (surface-rupturing) events is larger for normal faults, but peak slip rate is larger for thrust faults. After these initial studies of dip-slip faults, we moved on to model nonplanar fault systems. Figure 1 shows the fault geometry and loading method for a typical right-lateral 2D strike-slip faulting model with a change in strike half-way down the fault along strike. To supply the pre-stress for dynamic simulations, the material is sheared at a constant rate of 0.5 m/s at a distance of 200 km from the fault (with velocities damped to eliminate seismic waves in the loading process); the model space is large enough that the loading is uniform across the material. When failure is detected on the fault, loading is stopped and a dynamic rupture model (including full seismic wave field) is simulated. Figure 2 shows the shear and yield stresses on the fault just before and just after rupture for a sequence of six earthquakes. Note that since yield stress is directly proportional to normal stress, yield stress can be considered a proxy for normal stress. Also note that the shear and normal stress loading is the same for the two fault segments: the northern fault segment (with along-strike coordinates greater than 20 km) is at an angle of 20° to the loading, leading to an increased normal (yield) and decreased shear stress relative to the southern (loading-parallel) segment. After one event (the top-left frame), the initial relatively homogeneous stress becomes highly heterogeneous near the segment junction. The sense of slip on the fault leads to a decrease in normal stress (and thus frictional shear stress) on the southern segment, and an increase in this stress on the northern segment. Thus, the slip on the fault has greatly affected the stress field on the fault itself—it is no longer simply a regional stress field resolved onto the two segments.

The displacement and slip also have many features attributable to the specific geometry of the fault system. Figure 3 shows a sequence of fault displacements (for each side of the fault individually) and the total slip for the same earthquakes shown in Figure 2. The effect of the fault geometry can be seen in the first event (top-left frame), which displays higher slip on the loading-parallel southern segment than on the northern segment, which is less favorably oriented for rupture and slip. Furthermore, there is an asymmetry between the movement of the left wall (with the smaller angle) and the right wall (with the larger angle); the displacement of the left (west) wall is significantly larger than that of the right (east) wall.

After multiple earthquakes, an interesting pattern of rupture appears. The next three events all nucleate on the southern segment, in the area of reduced normal/yield stress near the segment boundary. Thus, the geometrical discontinuity appears to be a preferred nucleation region for this fault system. These first four earthquakes rupture the entire fault system. Different behavior is seen in the fifth event (bottom-middle panel in Figure 3. While this event nucleates in the same location as before, rupture does not propagate along strike to the second (non-parallel) segment. Rather, the geometrical discontinuity acts as a barrier to rupture. The next event ruptures the entire fault system again, and the increased stress buildup on the previously-skipped north segment leads to increased slip on that segment. In summary, we observe that through the addition of a change in strike, complexity in stress and slip result even with a simple slip-weakening friction law.

These simple results present a physical difficulty after multiple earthquake cycles. As seen in Figure 2, the stress buildup on the north segment and the stress decrease on the south segment build up over time, and become almost pathological after only a small number of events. Therefore, we conclude that our model is missing a physical mechanism of fundamental importance: a means by which to relax the stress buildup at the geometrical discontinuity. One possibility is the inclusion of a third fault at the segment intersection, as suggested by Andrews (1989). Another possibility is the inclusion of a form of viscoelastic creep or flow, such as that used in Freed and Lin (2001). Of course, segment boundaries in nature may not be as sharp as in our models, and we must address this issue in future models as well. Answering questions about the fate of stress buildups at geometrical discontinuities and fault intersections is the subject of proposed future work.

Andrews, D. J. (1989). Mechanics of fault junctions, *J. Geophys. Res.* **94,** 9389-9397.

Freed, A. M., and J. Lin (2001). Delayed triggering of the 1999 Hector Mine earthquake by viscoelastic stress transfer, *Nature* **411,** 180-183.

Oglesby, D. D. (1999). *Earthquake dynamics on dip-slip faults*, Ph. D. Thesis, University of California, Santa Barbara.

Whirley, R. G., and B. E. Engelmann (1993). *DYNA3D: A Nonlinear, Explicit, Three-Dimensional Finite Element Code for Solid and Structural Mechanics - User Manual*, University of California, Lawrence Livermore National Laboratory, UCRL-MA-1107254 Rev. 1.

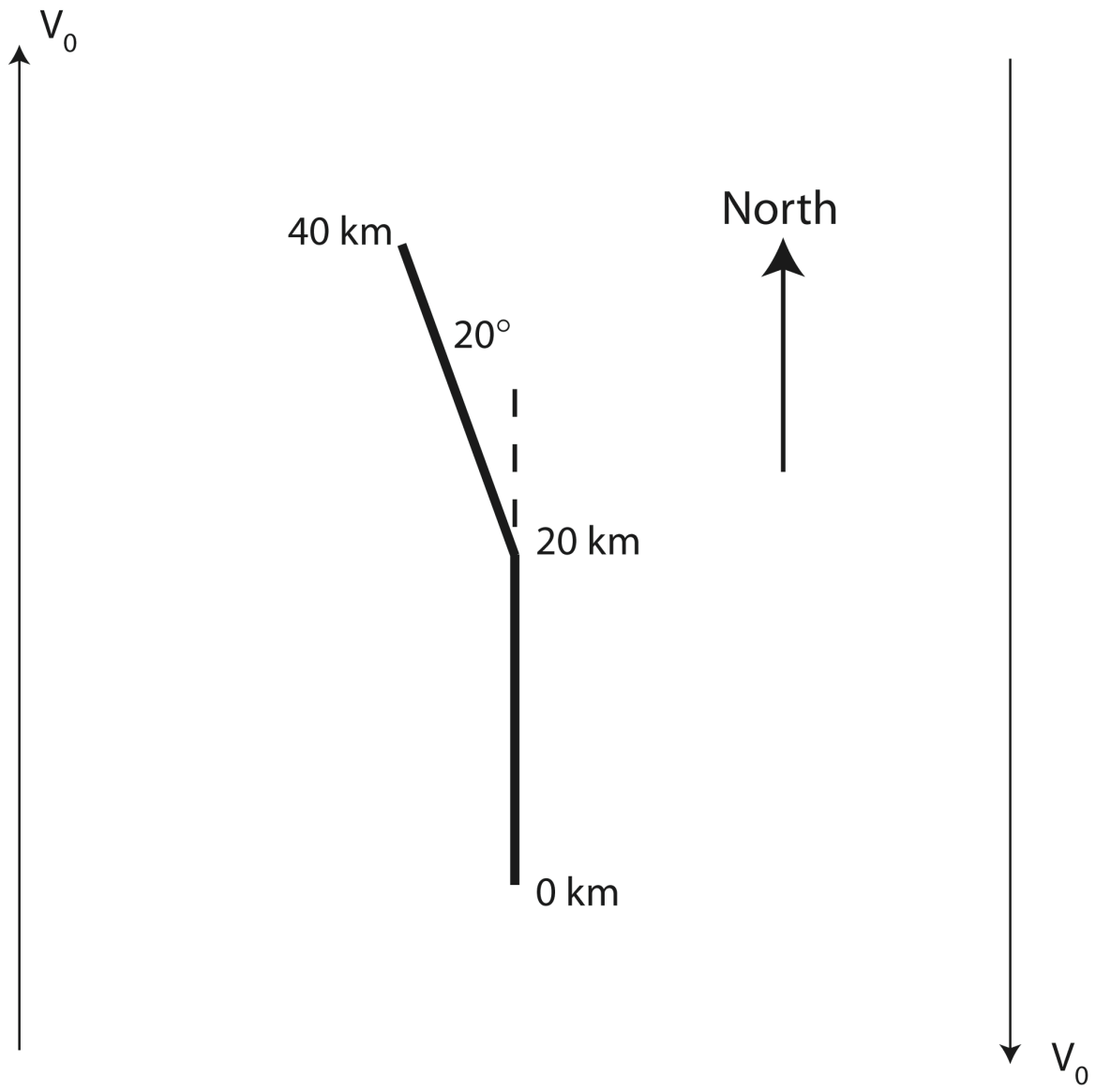

Figure 1. Map view of a 2D strike-slip fault with a change in strike at a distance of 20 km along strike. The fault is loaded by a constant velocity V_0 applied far from the fault in the interseismic period.

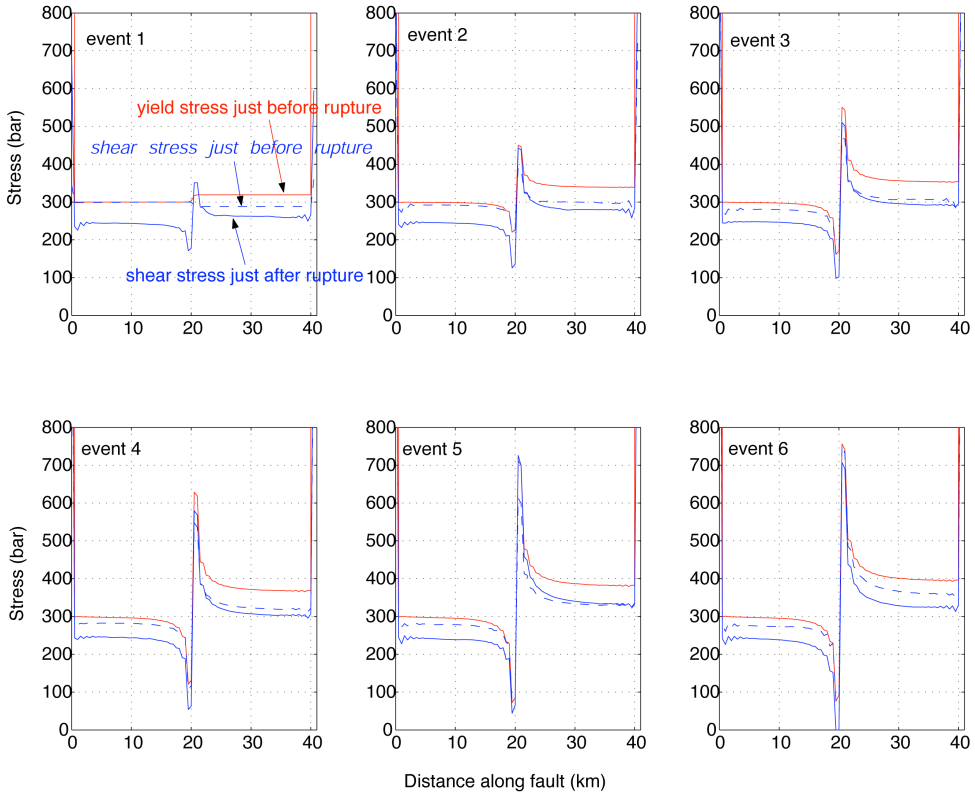

Figure 2. Evolution of shear and yield stress on fault system before and after six earthquakes. Note that yield stress is a proxy for normal stress. Along-strike distances between 0 and 20 km are on the southern segment (parallel to loading), and along-strike distances between 20 and 40 km are on the northern segment (20° from the loading).

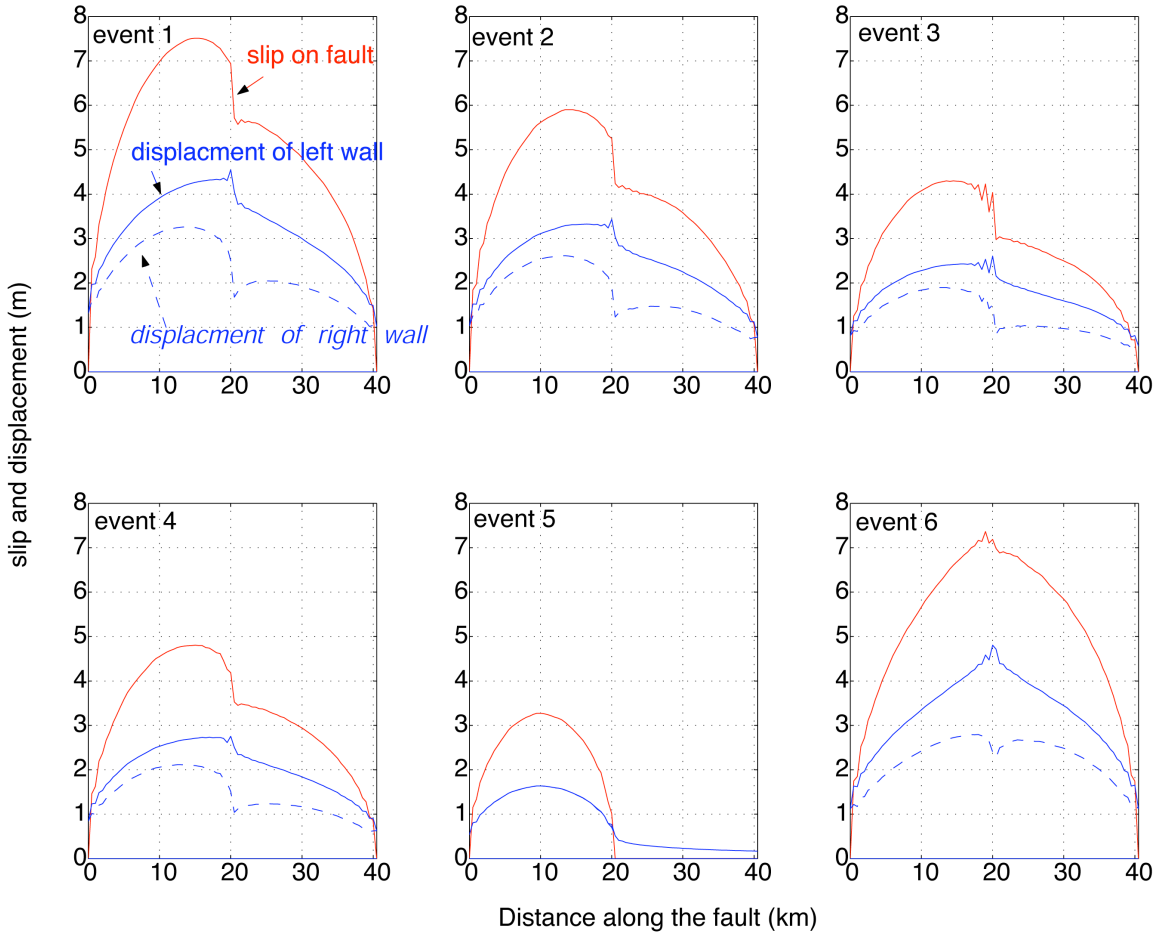

Figure 3. Evolution of slip and fault displacement over six earthquakes on fault system. The horizontal axis is the same as in Figure 2. For comparison, the absolute value of displacement is shown for both sides of the fault.